JOC Article

Effect of Alkyl Group Size on the Mechanism of Acid Hydrolyses of Benzaldehyde Acetals

Alexanders T. N. Belarmino,[†] Sandro Froehner,[‡] and Dino Zanette*

Departmento de Química, Universidade Federal de Santa Catarina, 88040-900, Florianópolis, Santa Catarina, Brazil

João P. S. Farah[§]

Instituto de Química, Universidade de São Paulo, C. Postal 26077, São Paulo-SP, 05599-970, Brazil

Clifford A. Bunton[||]

Department of Chemistry and Biochemistry, University of California, Santa Barbara, California 93106

Laurence S. Romsted[⊥]

Department of Chemistry and Chemical Biology, Wright & Rieman Laboratories, Rutgers, The State University of New Jersey, New Brunswick, New Jersey 08903

zanette@qmc.ufsc.br

Received April 29, 2002

Hydrolyses of benzaldehyde acetals, $PhCH(OR)_2$, are specific hydrogen-ion catalyzed when R = methyl, *n*-butyl, but with secondary and tertiary alkyl derivatives, R = *i*-propyl, *s*-butyl, *t*-butyl, *t*-amyl, hydrolyses are general-acid catalyzed. The Brønsted α values for both secondary and tertiary alkyl groups are in the range: α = 0.57−0.61. A simple iterative procedure was developed to estimate the individual rate constants for general-acid catalysis by the diacid and monoacid forms of succinic acid buffer. Plots of log k_{obs} (at [buffer] = 0 M) against pH are linear for the secondary and tertiary acetals, and plots of log k_H for the H_3O^+-catalyzed reaction, ^{13}C and ^1H chemical shifts, and $^1J_{CH}$ coupling constants against the Charton steric parameter, *ν*, for alkoxy groups are linear. The second-order rate constant, k_H, increases about 100-fold on going from R = Me to R = *t*-amyl, indicating the significant role of steric effects on reactivity. Steric effects upon ^{13}C NMR chemical shifts and coupling constants indicate that increasing the bulk of the alkoxy moiety increases the electron density at the carbon reaction center, which accelerates hydrolysis. Analysis of the Jencks−More−O'Ferrall free energy diagram for the reaction provides support for concerted proton transfer and C−O bond breaking in the transition state for hydrolyses of benzaldehyde acetals with secondary and tertiary alkyl groups in contrast to specific hydrogen catalysis with R = Me and *n*-Bu. All our results are consistent with rate-determining acid hydrolysis of benzaldehyde dialkyl acetals to hemiacetal intermediates that breakdown rapidly to benzaldehyde.

Introduction

Scheme 1 shows acid hydrolyses of benzaldehyde dialkyl acetals with primary, secondary, and tertiary alkyl groups in aqueous solution and the structures and abbreviations used for each dialkyl acetal. The overall reaction is reversible, but in dilute aqueous solutions it is driven to the carbonyl and alcohol products.[1−3]

Hydrolyses of many acetals are catalyzed specifically by the hydrogen ion, following the A-1 mechanism, as illustrated for benzaldehyde dialkyl acetals in Scheme 2.[1−4] For example, for acid-catalyzed hydrolyses of dimethyl, and diethyl, benzaldehyde acetals, the first step is considered to be equilibrium protonation followed by rate-limiting loss of alcohol to give oxocarbenium ions that, in water, give the final products in subsequent fast steps.[1−5] The observed first-order rate constants depend only on hydrogen-ion concentration with no catalysis by undissociated acids, i.e., by the acid form of a buffer.

* To whom correspondence should be addressed.
[†] E-mail: alexanders.atnb@dpf.gov.br.
[‡] E-mail: froehner@qmc.ufsc.br.
[§] E-mail: jpsfarah@usp.br.
[||] E-mail: bunton@chem.ucsb.edu.
[⊥] E-mail: romsted@rutchem.rutgers.edu.

(1) Carey, R. A.; Sundberg, R. J. *Advanced Organic Chemistry. Part A: Structure and Mechanism*, 3rd ed.; Plenum Press: New York, 1993.
(2) Lowry, T. H.; Richardson, K. S. *Mechanism and Theory in Organic Chemistry*, 3rd ed.; Harper and Row: New York, 1987.
(3) Cordes, E. H.; Bull, H. G. *Chem. Rev.* **1974**, *74*, 581−603.
(4) Fife, T. H. In *Advances in Physical and Organic Chemistry*; Gold, V., Bethell, D., Eds.; Academic Press: London, 1975; Vol. 11, pp 1−122.
(5) Buckley, N.; Oppenheimer, N. J. *J. Org. Chem.* **1996**, *61*, 8048−8062.

10.1021/jo0202987 CCC: $25.00
Published on Web 01/07/2003

SCHEME 1

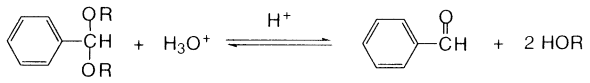

Abbreviations: R = CH_3–, Me, BMA; $CH_3(CH_2)_2CH_2$–, *n*-Bu, BBA; $(CH_3)_2CH$–, *i*-Pr, BIPA; $CH_3CH_2(CH_3)CH$–, *s*-Bu, BSBA; $(CH_3)_3C$–, *t*-Bu, BTBA; $CH_3CH_2(CH_3)_2C$–, *t*-Am, BTAA

SCHEME 2

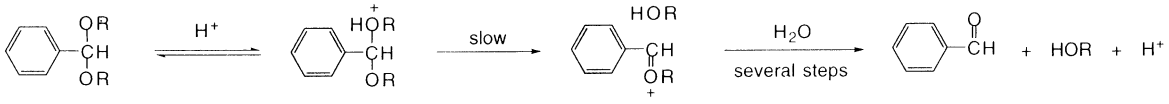

SCHEME 3

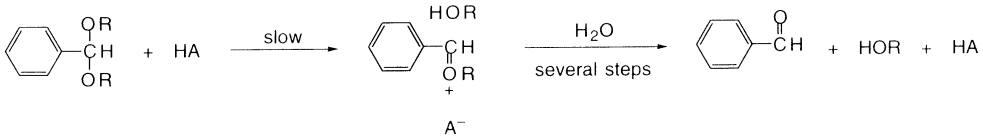

General-acid catalysis by buffer acids, illustrated for benzaldehyde dialkyl acetals in Scheme 3, is induced by various structural modifications of the acetal,[1−5] e.g., by enhancing the stability of the oxocarbenium ion and/or by releasing strain in the tetrahedral ground state.[1,6−8] There are also examples of intramolecular general-acid catalyses.[9,10] Ortho esters are structurally related to acetals and hydrolyses of some of them are general-acid catalyzed.[11] These reactions are models for hydrolyses at glycosidic linkages in biological systems.[5] With very good leaving groups, e.g., aryloxy, hydrolyses may be spontaneous,[5] which is mechanistically equivalent to the rapid hydrolyses of α-haloethers following the S_N1 mechanism.[12,13] Increasing the bulk of alkoxy groups of benzaldehyde acetals induces general-acid catalysis; e.g., the hydrolysis of BTBA is general-acid catalyzed (Scheme 3).[6] This mechanistic change is rationalized by assuming that the greater bulk of the *tert*-butoxy group inhibits protonation, but accelerates C−O cleavage, so that the two steps become concerted. General-acid-catalyzed reactions generally have Brønsted α values in the range $0 < \alpha < 1$.[14,15] Hydrolysis of BTBA in dilute strong acid is faster than those of the corresponding dimethyl and diethyl derivatives, and this rate enhancement has been ascribed to relief of steric strain in formation of the transition state.[1] An alternative mechanism, rate-determining acid-catalyzed loss of the *tert*-butyl cation, was excluded by determination of the position of bond cleavage by ^{18}O isotopic labeling.[16]

Changes in substrate conformation may also be important[5,17] because steric interactions involving both the alkoxy groups and an alkyl or aryl group at the reaction center will affect anomeric interactions between the unshared electron pairs of the oxygens.[18] Reducing the conformational change in going from the initial to the transition state, e.g., by changing the bulk of the alkoxy groups,[18] should favor reaction and lower the extent of proton transfer in the transition state. Evidence of steric effects on initial state conformations should be indicated by changes in ^{13}C and ^1H NMR chemical shifts and $^1J_{CH}$ coupling constants at the reaction center.[9] We combined these approaches with kinetic studies on the hydrogen-ion or buffer-mediated hydrolyses of the benzaldehyde dialkyl acetals listed in Scheme 1 with primary, secondary, and tertiary alkyl groups of various sizes. These acetals were selected because the structural changes should have minimal electronic effects. The hydrolyses of secondary and tertiary alkyl groups were carried out in various buffers, including succinic acid, for which we separated the contributions of the mono- and diacidic forms by two different methods. The results confirm a transition from specific to general-acid-catalyzed hydrolysis as the bulk of the alkoxy group increases. Because acetal hydrolyses involve both proton transfer to oxygen and breaking the carbon−oxygen bond, structural effects were analyzed by using a Jencks−More−O'Ferrall free energy diagram. Consideration of the energy barriers to the putative stepwise reactions is based on existing data on acid−base and carbenium-ion equilibria.

Finally, hydrolyses of primary benzaldehyde acetals show induction periods by stopped-flow spectroscopy for primary alkyl acetals that are too fast to be observed by

(6) Anderson, E.; Fife, T. H. *J. Am. Chem. Soc.* **1971**, *93*, 1701−1704.
(7) Craze, G.-A.; Kirby, A. J. *J. Chem. Soc., Perkin Trans. 2* **1978**, 354−356.
(8) Anderson, E.; Fife, T. H. *J. Am. Chem. Soc.* **1969**, *91*, 7163−7166.
(9) Fife, T. H.; Bembi, R.; Natarajan, R. *J. Am. Chem. Soc.* **1996**, *118*, 12956−12953.
(10) Brown, J. B.; Kirby, A. J. *J. Chem. Soc., Perkin Trans. 2* **1997**, 1081−1093.
(11) DeWolfe, R. H. *Carboxylic Ortho Acid Derivatives: Preparation and Synthetic Applications*; Academic Press: New York, 1970; Vol. 14.
(12) Buckley, N.; Maltby, D.; Burlingame, A. L.; Oppenheimer, N. J. *J. Org. Chem.* **1996**, *61*, 2753−2762.
(13) Knier, B. L.; Jencks, W. P. *J. Am. Chem. Soc.* **1980**, *102*, 6789−6798.
(14) Zuman, P.; Patel, R. *Techniques in Organic Reaction Kinetics*; Wiley: New York, 1984.
(15) Bell, R. P. *The Proton in Chemistry*; Cornell University Press: Ithaca, NY, 1959.
(16) Cawley, J. J.; Westheimer, F. H. *Chem. Ind. (London)* **1960**, 656−656.
(17) Li, S.; Kirby, A. J.; Deslongchamps, P. *Tetrahedron Lett.* **1993**, *34*, 7757−7758.
(18) Anderson, J. E.; Heki, K.; Hirota, M.; Jorgensen, F. S. *J. Chem. Soc., Chem. Commun.* **1987**, 554−555.

TABLE 1. Second-Order Rate Constants, k_H and k_{HA}, for the Acid-Catalyzed Hydrolyses of Dialkyl Benzaldehyde Acetals at 25 °C in Aqueous Buffers with 0.5 M KCl

acetal	buffer (pH),[b] no. of data pts, r = linear correlation coefficient	k_H, $M^{-1}\,s^{-1}$	k_{HA}, $M^{-1}\,s^{-1}$ [a]
BMA (Me)[c]	succinate (4.50, 4.90), 8 pts	21.3± 2.3%	
BBA (*n*-Bu)[c]	succinate (4.50, 4.90), 8 pts	78.3 ± 0.38%	
BIPA (*i*-Pr)	formate (3.60, 4.20, 4.50), 15 pts, $r = 9971$	176	0.129
	acetate (4.49, 4.70, 5.15), 15 pts, $r = 9920$	244	0.0266
BSBA (*s*-Bu)	formate (3,55, 4.10), 8 pts, $r = 0.9957$	161	0.170
	acetate (4.50, 5.00), 8 pts, $r = 0.9978$	245	0.0323
BTBA (*t*-Bu)[c]	formate (3.60, 4.20, 4.50), 15 pts, $r = 9977$	2080	3.04
	acetate (4.49, 4.70, 5.15), 15 pts, $r = 0.9968$	2450	0.358[c]
	phosphate (6.60, 7.10), 10 pts, $r = 0.9996$	2560	0.0308[c]
BTAA (*t*-Am)	acetate (4.60, 5.00), 10 pts, $r = 0.9996$	2110	0.556
	phosphate (6.60, 7.10) 10 pts, $r = 0.9999$	2530	0.0610

[a] Values for k_{HA} obtained by using eq 2 (see text). [b] Buffer pK_a values: formate, 3.85; acetate, 4.75; phosphate, 6.75; succinate (H_2A), 4.21; succinate (HA^-), 5.64 (ref 25). [c] Literature values (25 °C, $M^{-1}\,s^{-1}$): BMA, 60.5 (ref 19); BBA, 73 (ref 24); BTBA, 2000 (ref 24); BTBA, $k_H = 2950$, $k_{HA} = 0.325$; acetate, 0.029; phosphate (ref 6).

TABLE 2. Second-Order Rate Constants, k_H, k_{H_2A}, and k_{HA}, for the General-Acid-Catalyzed Hydrolyses of Secondary and Tertiary Dialkyl Benzaldehyde Acetals at 25 °C in Succinate Buffers with 0.5 M KCl[a]

acetal	succinate form (pH), no. of data pts, r = linear correlation coefficient	k_H, $M^{-1}\,s^{-1}$	k_{H_2A} or k_{HA}, $M^{-1}\,s^{-1}$
BIPA (*i*-Pr)	H_2A, I (4.21), 10 pts, $r = 0.9753$	200	0.109
	HA^-, I(5.10, 5.40), 10 pts, $r = 0.7625$		0.00421
	H_2A, II (4.21, 4.50), 10 pts., $r = 0.9994$	207[b]	0.116
	HA^-, II (5.40, 80 & 100 mM buffer), av 2 pts		0.0144
BSBA (*s*-Bu)	H_2A, I (4.01, 4.56), 10 pts, $r = 0.9767$	221	0.106
	HA^-, I (5.10, 5.40) ,10 pts, $r = 0.9711$		0.00608
	H_2A, II (4.01, 4.56), 10 pts, $r = 0.9710$	209[c]	0.119
	HA^-, II (5.40, 80 & 100 mM buffer), av 2 pts		0.0144
BTBA (*t*-Bu)	H_2A, I(4.67), 5 pts, $r = 0.9996$	1920	1.62
	HA^-, I (5.50, 5.73), 10 pts, $r = 0.9332$		0.0785[f]
	H_2A, II (4,67), 5 pts, r= 0.9997	2260[d]	1.71
	HA^-, II (5.50, 5.73), 10 pts, $r = 0.8927$		0.0584[f]
BTAA (*t*-Am)	H_2A, I (4.67, 5.01), 10 pts, $r = 0.9873$	2080	2.51
	HA^-, I (5.69, 5.91), 10 pts, $r = 0.9759$		0.164
	H_2A, II (4.67, 5.01), 8 pts, $r = 0.9858$	2240[e]	2.55
	HA^-, II (5.69, 5.91), 10 pts, $r = 0.9803$		0.158

[a] Values of k_{H_2A} and k_{HA} Calculated by methods I and II. Method I: k_H, k_{H_2A}, and k_{HA} obtained by the iteration method. Method II: k_{HA} obtained by difference; $k_{obs} - k_H(av)[H_3O^+] - k_{H_2A}[H_2A]$. See text for details. [b] $k_H = (244 + 176 + 200)/3 = 207\ M^{-1}\,s^{-1}$. [c] $k_H = (161 + 245 + 220)/3 = 209\ M^{-1}\,s^{-1}$. [d] $k_H = (1920 + 2080 + 2450 + 2600)/4 = 2260\ M^{-1}\,s^{-1}$. [e] $k_H = (2110 + 2530 + 2080)/3 = 2240\ M^{-1}\,s^{-1}$. [f] Literature value of k_{HA} (25 °C $M^{-1}\,s^{-1}$, succinate buffer) for BTBA 0.237 (ref 6). [g] Buffer pK_a values: see Table 1.

conventional methods.[19,20] These short induction periods are attributed to formation of transient hemiacetal intermediates within the first few seconds of the reaction and do not perturb the relatively slow overall hydrolyses. However, Jensen[21,22] and co-workers and Capon[23] report significant induction periods (1−2 min) for some primary acetals and significant deviations from first-order kinetics in the pH range 5−7 for the hydrolysis of BTBA, a break in the log k_{obs}−pH profile for BTBA, and a marked increase, by a factor of approximately 10, in the observed second-order rate constant for BTBA hydrolysis at pH > 7. They conclude that at a low pH, ca. ≤5, the rate-determining step is a breakdown of the hemiacetal intermediate (second step in Scheme 3), followed by a transition to rate-determining acetal hydrolysis above pH 7. We see no break in the log k_{obs}−pH profiles for any hydrolyses, in particular those of the tertiary acetals, BTBA and BTAA. In sum, all our results are consistent with rate-determining acid hydrolysis of primary, secondary, and tertiary benzaldehyde dialkyl acetals, followed by rapid breakdown of the hemiacetal intermediate to benzaldehyde.

Results

Kinetics. Tables 1 and 2 list all the second-order rate constants ($M^{-1}\,s^{-1}$) for hydronium ion, k_H, and buffer-catalyzed hydrolyses, k_{HA} and k_{H_2A}, of benzaldehyde acetals at 25 °C in 0.5 M KCl. Table 1 lists second-order rate constants, k_H, for hydrolyses of BMA and BBA in formate, acetate, and phosphate buffers. Table 2 lists estimates of second-order rate constants for buffer-catalyzed hydrolyses by succinic acid, H_2A, and its monoanion, HA^-, obtained by methods I and II (see Appendix). All values of the observed first-order rate constants, k_{obs}, obtained at each buffer concentration and pH that were used to calculate the second-order rate constants are compiled in the Supporting Information. Values of k_{obs} are averages of three kinetic runs and were determined in 3−4 different buffers across a concentra-

(19) Engell, K. M.; McClelland, R. A.; Sorensen, P. E. *Can. J. Chem.* **1999**, *77*, 978−989.
(20) Findley, R. L.; Kubler, D. G.; McClelland, R. A. *J. Org. Chem.* **1980**, *45*, 644−648.
(21) Jensen, J. L.; Martinez, A. B.; Shimazu, C. L. *J. Org. Chem.* **1983**, *48*, 4175−4179.
(22) Jensen, J. L.; Lenz, P. A. *J. Am. Chem. Soc.* **1978**, *100*, 1291−1293.
(23) Capon, B. *Pure Appl. Chem.* **1977**, *49*, 1001−1007.

tion range of 10−250 mM buffer at several different pH values. Where comparable, second-order rate constants are in reasonable agreement with literature values[6,24] (see Tables 1 and 2). Our value of k_{HA} for BTBA in hydrogen succinate buffer is lower than earlier values (see Table 2), but these values probably included minor contributions from catalysis by succinic acid, because catalysis by the two acid forms had not been separated (see below).

Hydrolyses of BMA and BBA are not buffer catalyzed up to 0.25 M succinate. Reactions are first-order in $[H^+]$ and values of k_H in Table 1 are averages of eight sets of rate data. Note: square brackets indicate concentration in molarity here and throughout the text.

Hydrolyses of the other acetals are catalyzed by the acid form of the buffer, Tables 1 and 2, and by H_3O^+. For reactions in formate, acetate and phosphate buffers, the relationship of k_{obs} to acid concentration is given by

$$k_{obs} = k_H[H^+] + k_{HA}[HA] \quad (1)$$

Values of the two rate constants were obtained from the slope, k_{HA}, and intercepts, k_H, of data plots based on

$$\frac{k_{obs}}{[H^+]} = k_H + \frac{k_{HA}[HA]}{[H^+]} \quad (2)$$

Figure 1 shows a typical plot of this type for hydrolysis of BTBA in formate buffer at pH 3.6, 4.2, and 4.5. For all the substrates, correlation coefficients for such plots are ≥0.992 (Table 1).

For reactions in succinate buffers (Table 2), k_{obs} is given by

$$k_{obs} = k_H[H^+] + k_{H_2A}[H_2A] + k_{HA}[HA^-] \quad (3)$$

Contributions by H_2A and HA^- to k_{obs} were separated by working over a significant pH range and using literature values of the first and second dissociation constants of $pK_a(1) = 4.21$ and $pK_a(2) = 5.64$[25] and by assuming that these values are insensitive to ionic strength up to 0.5 M KCl. To check this assumption, we measured pK_a of formic and acetic acid under our kinetic conditions, i.e., 0.5 M KCl (see Experimental Section), and obtained 3.89 and 4.74, which are similar to the literature values, respectively, of 3.85 and 4.75[25] and support our assumption that pK_a values of all the buffers are insensitive to ionic strength.

Values of k_{H_2A} and k_{HA} for catalysis by succinic acid and succinate monoanion were estimated by methods I and II, which are fully described in the Appendix. Method I is an iterative process in which initial estimates of k_{H_2A} and k_{HA} are made by using equations similar to eq 2 for H_2A and HA^- at a pH at which H_2A or HA^- is the dominant form of the buffer. Initial estimates of k_{H_2A} and k_{HA} are then substituted into equations that contain terms that include both rate constants, the acidity constants $K_a(1)$ and $K_a(2)$ for ionization of succinic acid and concentrations of both forms of the buffer, H_2A and HA^-. The concentrations of H_2A and HA^- at each pH are obtained by solving quadratic equations that contain the acidity constants $K_a(1)$ and $K_a(2)$. An iterative procedure was used to solve for the two rate constants until their values converged, which usually took four iterations. Figure 2 shows the results for BTBA in succinic acid. The value of Y for the ordinate contains several terms including k_{obs} and is different for plots A and B in Figure 2 (see caption). The definitions of Y are in the Appendix. These results show that values of k_{H_2A} are generally better defined, i.e., less scatter in the data, than those of k_{HA}, which is true for BTBA (Figure 2) and the other acetals (see correlation coefficients in Table 2). The primary reason for the greater scatter in the estimates and uncertainty of the values of k_{HA} is that they are an order of magnitude smaller than those of k_{H_2A}.

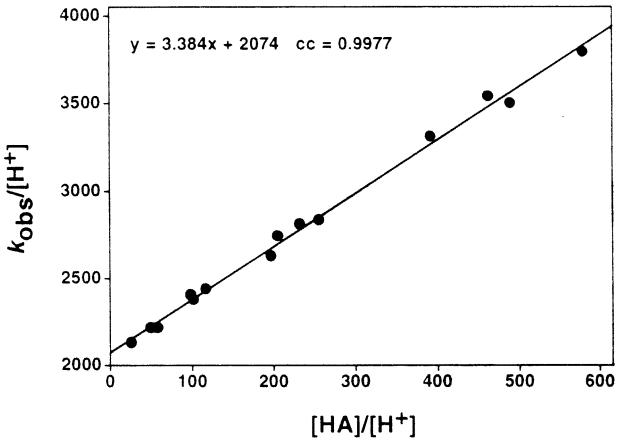

FIGURE 1. Plot of $k_{obs}/[H^+]$ versus $[HA]/[H^+]$ based on eq 2 for BTBA in formate buffer at pH 3.60, 4.20, and 4.50. Values of k_H and k_{HA} were estimated from the slopes and intercepts, respectively, of the least-squares fit, correlation coefficient: cc = 0.9977 (see inserted equation).

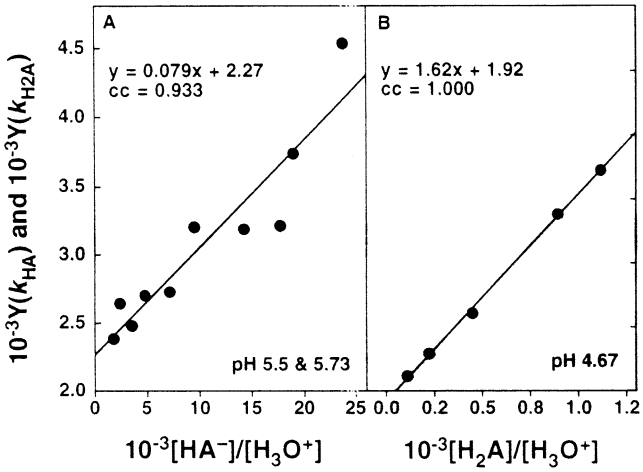

FIGURE 2. Plots of Y values (see text and Appendix) for the acid-catalyzed hydrolysis of BTBA in succinic acid buffer as a function of buffer−hydronium concentration ratios at 25 °C. Plots are from the fourth (last iteration) used to estimate final values of k_{HA} (A) and k_{H_2A} (B). The insets indicate the pH of the buffers and the fitting equation and correlation coefficient, cc, used to estimate k_H from the intercepts (plots A and B) and k_{HA} (plot A) and k_{H_2A} (plot B).

(24) Froehner, S. J.; Nome, F.; Zanette, D.; Bunton, C. A. *J. Chem. Soc., Perkin Trans. 2* **1996**, 673−676.

(25) Kortum, G.; Vogel, W.; Andrussow, K. *Dissociation Constants of Organic Acids in Aqueous Solution*; Butterworth: London, 1961.

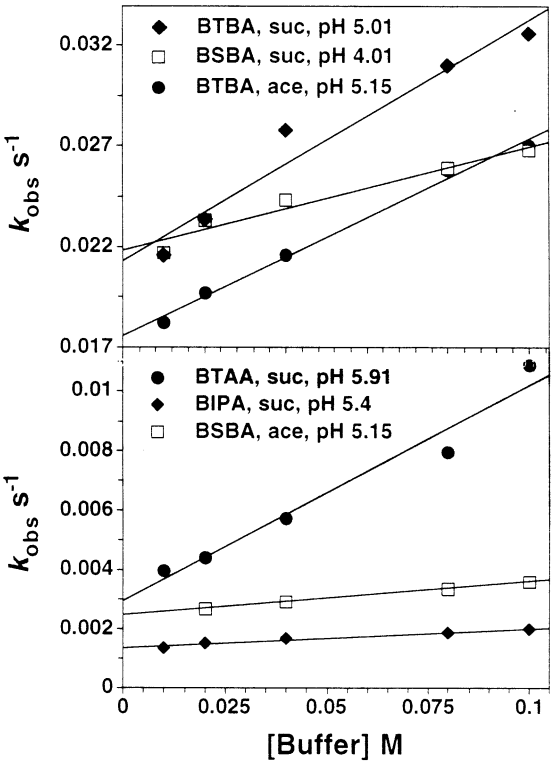

FIGURE 3. Effect of increasing [buffer] on k_{obs} for the buffer-catalyzed hydrolyses of secondary and tertiary acetals at constant pH, 0.5 M KCl at 25 °C. The acetal and buffer types and pH for each data set are indicated in the figure. Lines are least squares correlations and were used to obtain k_{obs} at [buffer] = 0 M; see Figure 4.

Method II was used to check the results obtained by method I. In this approach, values of k_{H_2A} were estimated first at the lower pH by assuming that $k_{HA}[HA^-] \approx 0$, that k_H was best defined by the average of k_H values from plots of eq 1 for the other buffers, and then estimates of k_{H_2A} were obtained from slopes of plots of $k_{obs} - k_H(av)$-$[H_3O^+]$ against $[H_2A]$. This value of k_{H_2A} was used to obtain estimates of k_{HA} from similar plots that include terms for $[HA^-]$ at higher pH values. Table 2 summarizes the results from method II, pH values of the buffers used for each calculation, and the correlation coefficients. As with method I, correlation coefficients in method II are usually better for k_{H_2A} than for k_{HA}. The value of k_{HA} for BSBA by method II is the least well-defined because only two data points at the highest buffer concentration gave reasonable values of k_{HA} due to errors caused by small differences between two large numbers in the subtraction. For the remaining buffers, however, values of k_{H_2A} and k_{HA} by methods I and II are in reasonable agreement.

Correlations of log k_{obs} (at [buffer] = 0 M) against pH (Figure 4) were obtained by extrapolating plots of k_{obs} against [buffer], which gives values of the first-order rate constants of the hydrogen-ion-catalyzed reactions at the appropriate pH. Data are in the Supporting Information. Figure 3 shows six example plots, including four with the poorest correlation coefficients, and two with much better correlation coefficients. Table 3 summarizes the slopes, intercepts, and correlation coefficients, for each least-squares fit in Figure 3. Table 3 also summarizes the mean correlation coefficients and standard deviations for all k_{obs}−[buffer] plots obtained for each acetal. Note that the mean correlation coefficients are between 0.99 and 0.999.

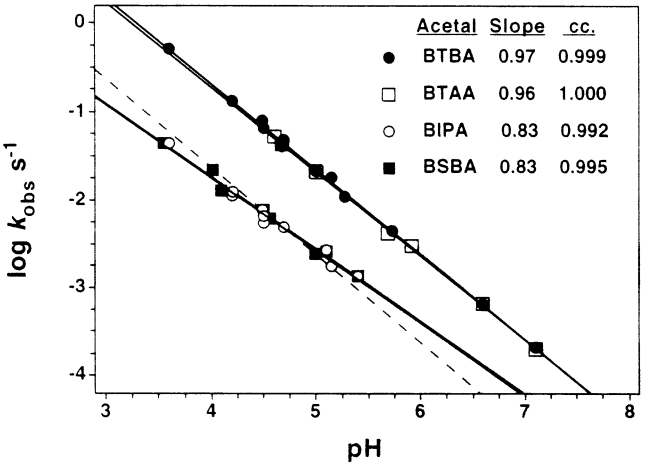

FIGURE 4. log k_{obs} ([buffer] = 0 M)−pH profiles for the secondary and tertiary acetals. Values of k_{obs} were obtained by extrapolation from intercepts of k_{obs}−[buffer] profiles, e.g., Figure 3. Solid lines are least-squares fits with the slopes and correlation coefficients listed in this figure. The dashed line has a slope of 1 positioned to intersect as many secondary acetal data points as possible.

TABLE 3. Fitting Parameters, Slopes, Intercepts, and Correlation Coefficients for k_{obs}−[Buffer] Plots from the Fits for the Representative Data in Figure 3, Mean Correlation Coefficients and Standard Deviations for All k_{obs}−[Buffer] Plots for BIPA, BSBA, BTAA, and BTBA Used To Create Figure 4[a]

acetal (pH)[b]	slope	intercept	corr coef
BTBA (5.01	0.120	0.021	0.977
BSBA (4.01)	0.051	0.022	0.975
BTBA (5.15)	0.098	0.018	0.996
BTAA (5.91)	0.073	0.029	0.981
BIPA (5.40)	0.0067	0.0013	0.988
BSBA (5.15)	0.011	0.0025	1.000

acetal[c]	no. of plots	mean corr coef	std dev
BIBA	10	0.996	0.004
BSBA	8	0.994	0.008
BTAA	9	0.997	0.003
BTBA	12	0.995	0.006

[a] Complete data sets in the Supporting Information. [b] From least-squares fits of data in Figure 3. Corr coef = correlation coefficient, Std. Dev. = standard deviation. [c] Least squares data on k_{obs}−[buffer] plots used to calculate log k_{obs} values at each pH.

Figure 4 shows that for all substrates and buffers, plots of log k ([buffer] = 0 M) against pH are linear with slopes ca. 0.96 for the tertiary and about 0.83 for the secondary acetals. Note that the slopes for the two tertiary and the two secondary acetals are essentially the same. The dashed line shows an imposed slope of −1.0 on the data for the secondary acetals. Because the buffers involve different anions, deviations from unit slopes are probably due to specific salt effects, even though we used 0.5 M KCl as a "swamping" electrolyte. Changing ion type may affect estimates of hydrogen-ion activity, or concentration, from use of a glass electrode, and also reaction rates. Specific salt effects have been observed in hydrolyses of acetals and ortho esters catalyzed by dilute strong acids,

TABLE 4. Brønsted α Values for Secondary and Tertiary Dialkyl Benzaldehyde Acetals at 25 °C in Aqueous Buffers with 0.5 M KCl Obtained by Methods I and II[a]

acetal	α (H_3O^+)	cc[d]
	Secondary	
BIPA, I[b]	0.61	0.9944
BIPA, II[c]	0.58	0.9969
BSBA, I[b]	0.60	0.9968
BSBA, II[c]	0.57	0.9981
	Tertiary	
BTBA, I[b]	0.60	0.9926
BTBA, II[c]	0.61	0.9910
BTAA, I[b]	0.57	0.9994
BTAA, II[c]	0.57	0.9994

[a] Values of α including k_H for the H_3O^+-catalyzed reaction and a statistical correction of a −0.3 for H_2A and $H_2PO_4^-$. [b] Method I (see text). [c] Method II (see text). [d] Linear correlation coefficient.

where there is no uncertainty in hydrogen-ion concentration.[26,27] These medium effects inevitably complicate comparisons of rate data from experiments with different buffers and "swamping" electrolytes. In this context we note that Jensen et al.[21] reported a break in plots of extrapolated values of log *k* against pH for hydrolysis of BTBA in acetate, cacodylate, and methylphosphonate buffers, which they ascribe to a change of mechanism from to rate-determining acetal hydrolysis to rate-determining breakdown of the hemiacetal.[21] Jensen et al. also report nonlinearity in the double reciprocal plots (as in eq 2 and Figures 1 and 2 here) used to estimate the rate constant for buffer catalysis of BTBA hydrolysis in cacodylate buffer between pH 6−7.[21] All our double reciprocal plots for secondary and tertiary acetals are linear at all pH values, although some contain scatter, e.g., Figure 2. Also, Anderson and Fife[6] obtained linear k_{obs}−[buffer] plots, as we do in Figure 3. On the basis of the linearity of our log *k*−pH plots for BTBA and BTAA in Figure 4, the overall consistency of our results, and the evidence of specific electrolyte effects on acetal hydrolyses,[26,27] we suspect that the reported break in the log *k*−pH profile and the nonlinearity of their buffer plots in cacodylate buffer reported by Jensen et al. as evidence for the buildup of hemiacetal intermediate in the hydrolysis of BTBA may be caused by a specific electrolyte effect.[21] There is also the possibility of decomposition of BTBA, which generates impurities and may complicate determination of rate constants (see Experimental Section).

To estimate α for the general-acid-catalyzed reactions, four different Brønsted plots were prepared for each acetal from the rate constants listed in Tables 1 and 2, i.e., plots with and without the value of k_H for the H_3O^+-catalyzed reaction and plots with and without the statistical correction for succinic acid, H_2A, and phosphate monoanion, $H_2PO_4^-$, which as dibasic acids can donate two protons. Literature pK_a values were used in the calculations and, as is standard practice, we assume that the pK_a of H_3O^+ is −1.74 and that at constant ionic strength, −log [H^+] = pH. The value of k_H(av) used in the Brønsted plots is the average obtained in different

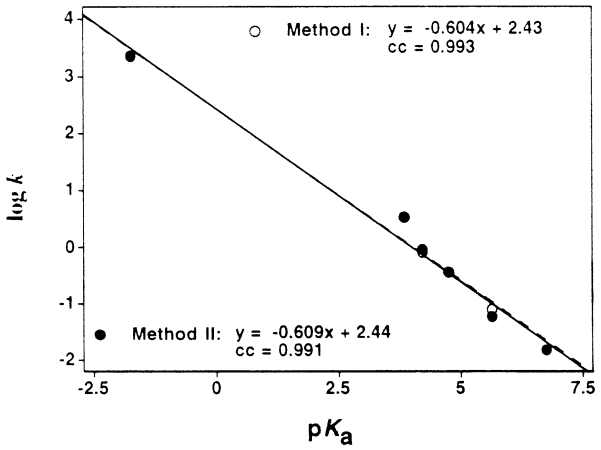

FIGURE 5. Typical Brønsted plot used to estimate α, showing results for BTBA from both method I and method II including the correlation coefficient, cc.

TABLE 5. ^{13}C and ^1H NMR Chemical Shifts and C−H Coupling Constants in $CDCl_3$ at 25 °C, the Steric Parameter, Average Second-Order Hydronium Ion Rate Constants, and Logarithms of the Second-Order Rate Constants Ratios Relative to BMA at 25 °C in 0.5 M KCl

acetal	$^{13}C^a$ δ (ppm)	$^1H^a$ δ (ppm)	$^1J_{CH}$ (Hz)	ν^b	k_H(av),[c] M^{-1} s^{-1}	log(k_H^R/k_H^{Me})
BMA	102.7	5.40	166.8	0.36	21.3	0
BBA	101.8	5.49	166.7	0.58	78.3	0.565
BIPA	99.8	5.58	162.7	0.75	207	0.988
BSBA	99.7	5.56	162.4	0.86	209	0.992
BTBA	94.2	5.71	158.7	1.22	2260	2.03
BTAA	93.0	5.73	156.5	1.35	2240	2.02

[a] Complete ^{13}C and ^1H data in Supporting Information. [b] Specifically for alkoxy groups from refs 28 and 29. [c] From Tables 1 and 2.

buffers (see footnotes to Table 2). The α values calculated by these four separate methods are summarized in the Supporting Information. Table 4 includes only the α values that include both average k_H values and the statistical correction. Figure 5 shows the Brønsted plots for BTBA obtained from Methods I and II. When average values of k_H for the H_3O^+-catalyzed reactions are excluded from the Brønsted plots, numerical values of α are higher than when k_H is included and spreads in α are greater. When the statistical corrections are excluded, there is a small change in α of about 0.02−0.05 log units. However, in all four cases there is no significant difference between α values for the secondary and tertiary acetals. In view of complications by specific salt effects of the buffer ions (see above), we believe that this is the significant conclusion regarding effects of secondary and tertiary alkyl groups on general-acid-catalyzed reactions of dialkyl benzaldehyde acetals despite differences in steric bulks.

Table 5 lists ^{13}C and ^1H NMR chemical shifts and $^1J_{CH}$ coupling constants at the reaction center, Charton steric parameters for alkoxy groups, ν,[28,29] average values of rate constants for acid hydrolysis, k_H(av), and the log ratio of the rate constants for each substrate relative to BMA, log(k_H^R/k_H^{Me}). Figure 6 shows plots of ^{13}C and ^1H

(26) Bunton, C. A.; Reinheimer, J. D. *J. Phys. Chem.* **1970**, *74*, 4457−4464.
(27) McIntyre, D. M.; Long, F. A. *J. Am. Chem. Soc.* **1954**, *76*, 3243−7.
(28) Charton, M. *J. Org. Chem.* **1978**, *43*, 3995−4001.
(29) Charton, M. In *Similarity Models in Organic Chemistry, Biochemistry and Related Fields*; Zalewski, R. I., Kryowski, T. M., Shorter, J., Eds.; Elsevier: Amsterdam, 1991; Vol. 42, pp 629−688.

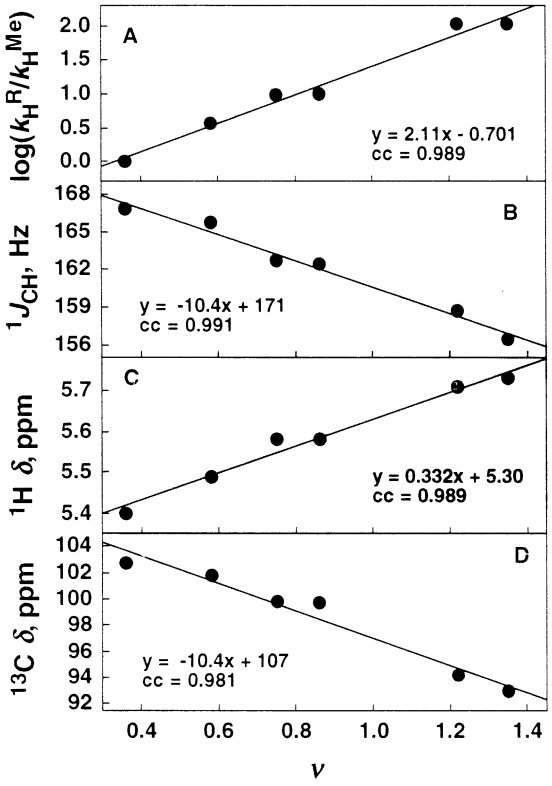

FIGURE 6. Correlation of the Charton steric parameter, ν, with the log of relative rate constants (to methoxy), A, with the C−H coupling constant, B, and proton, C, and carbon, D, chemical shifts at the central acetal carbon at 25 °C. The equations are linear least-squares fits of the data showing slopes, intercepts, and correlation coefficients.

chemical shifts, $^1J_{CH}$ coupling constants, and $\log(k_H^R/k_H^{Me})$ values versus ν. The four data sets were also plotted against a variety of other steric parameters, E_s, E_s', E_s*, and E_s^c, and Charton's ν for alkyl groups (not shown).[30] Correlation coefficients for all the experimentally measured values of steric bulk are generally ≥0.91 for each parameter, showing that all four experimental properties depend similarly on steric bulk. Figure 6 shows only the results for ν for alkoxy groups, cc ≈ 0.99, because this correlation is mostly closely related to substrate structures, i.e., to calculated molecular volumes of alkoxy groups based on van der Waals radii.[28,29] Note that steric effects are substantial because k_H(av) increases by 2 orders of magnitude in going from methyl (BBA) to *t*-Am (BTAA) derivatives.

Discussion

Failure to observe general-acid catalysis, as in hydrolyses of BMA and BBA, is necessary, but not sufficient, evidence that reaction involves preequilibrium protonation. As α → 1, the contribution of the $k_H[H^+]$ term to k_{obs}, eq 1, becomes so great that catalysis by HA is almost undetectable. Going to high buffer concentrations is not feasible because they may introduce adventitious, and specific, electrolyte effects.[26,27] In practice, demonstrating general-acid catalysis at α > 0.8 is difficult.[15] Conceivably, hydrolyses of all our acetals follow a common S_E2 mechanism in which protonation on oxygen is concerted with C−O cleavage, but for hydrolyses of BMA and BBA, oxygen protonation is essentially complete in their transition states. This ambiguity may be common for many specific hydrogen-ion-catalyzed reactions, except where substrate protonation is observed independently.[31] However, it is generally assumed that acetals of simple aliphatic aldehydes hydrolyze by A-1 mechanisms.[1−4]

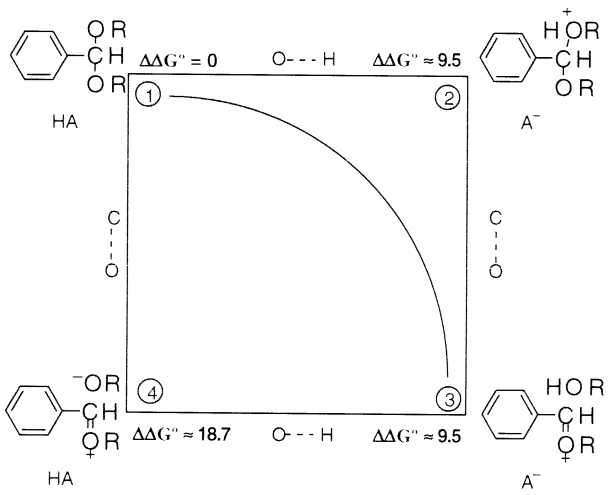

FIGURE 7. Jencks−More−O'Ferrall diagram for the acid hydrolysis of a benzaldehyde dialkyl acetal in aqueous solution at 25 °C. Corner 1 represents the initial state, corner 2 the intermediate from preequilibrium protonation, corner 3 the oxocarbenium ion intermediate, and corner 4 the oxocarbenium ion/alkoxide intermediates from initial cleavage of the C−O bond. The vertical axes represent C−O bond cleavage and the horizontal axes represent O−H bond formation from the initial state. Corners 2−4 also include estimates of the free energy difference $\Delta\Delta G°$ relative to that of the initial state, corner 1, $\Delta G° = 0$.

Structural changes caused in acetals by adding a phenyl ring, i.e., by going from aliphatic aldehyde to benzaldehyde acetals, may induce significant changes in mechanism and the role of catalyzing acids. The oxygens on benzaldehyde acetals should be less basic that those of aliphatic aldehyde acetals because inductive electron withdrawal by the phenyl group at saturated carbon inhibits preequilibrium proton transfers. However, the phenyl group should stabilize both oxocarbenium ion intermediates[3−5] and oxocarbenium ion-like transition states.[3,4] Sufficient stabilization should lead to slow proton transfer probably concerted with C−O bond cleavage and observable general-acid catalysis. Increasing the bulk of the alkoxy groups should also inhibit protonation on oxygen by reducing hydration of the developing oxonium ion. Thus, there is concerted proton transfer with some combination of a good leaving group, generation of a very stable oxocarbenium ion, and electronic and steric effects inhibiting proton transfer to oxygen.[5]

Analysis of substituent effects in terms of a Jencks−More−O'Ferrall free energy diagram, is illustrated in Figure 7.[2,32,33] The diagram shows only the step(s)

(30) Isaacs, N. S. *Physical Organic Chemistry*; Longman Group: Essex, U.K., 1987.

(31) Cox, R. A. *Acc. Chem. Res.* **1987**, *20*, 27−31.
(32) More O'Ferrall, R. A. *J. Chem. Soc. B* **1970**, 274−277.
(33) Jencks, W. P. *Chem. Rev.* **1972**, *72*, 705−718.

generating the oxocarbenium ion (Schemes 2 and 3), because in water with dilute substrate, formation of the oxocarbenium ion is rate limiting.[2] The two stepwise pathways along the axes from the reactant corner, 1, are (a) the classical A-1 mechanism of initial protonation followed by C−O cleavage or (b) initial C−O cleavage followed by rapid protonation of the alkoxide ion, i.e., spontaneous (uncatalyzed) hydrolysis.[5]

We estimated the free energies differences, $\Delta\Delta G°$ values, of hypothetical intermediates at corners 2−4, relative to the initial state, corner 1, $\Delta G° = 0$ at the standard state of 1 M BMA and 1 M hydronium ions at 25 °C from the equation $\Delta\Delta G° = -RT \ln K$, with $R =$ 0.001 987 kcal K^{-1} M^{-1} and $T = 298.15$ K (25 °C). $\Delta\Delta G°$ for protonation of the acetal, corner 1, BMA, to its conjugate acid, corner 2, is given by the pK_a of the conjugate acid, ca. −7,[3,34] and $\Delta\Delta G° \approx 9.5$ kcal/mol. The free energy difference between corner 4 and the oxocarbenium ion product, corner 3, is given by the pK_a of MeOH, which is 15.5,[35] and $\Delta\Delta G°$ (corner 3 to 4) ≈ 9.2 kcal/mol. The free energy difference between the product corner, 3, and the initial state, corner 1, is more difficult to estimate because it includes proton transfer and C−O bond cleavage of an aryl alkyl ether. We made an estimate from pK_{R+} for conversions of arylmethyl carbocations into ROH and H_3O^+ (Scheme 4). This hydration reaction is similar to the transformation of the oxocarbenium ion and HOR, corner 3, into the acetal and H_3O^+, corner 1. Some values of pK_{R+} are Ph_3C^+, −6.6; 4-Me$OC_6H_4CPh_2^+$, −3.4, $(4\text{-MeO}C_6H_4)_2CH^+$, −5.7.[36] We assume that for formation of an oxocarbenium ion pK_{R+} is ca. −3, i.e., that the electronic release from the two alkoxy groups is similar to that from two phenyl and one 2-methoxyphenyl groups, and that pK_{R+} is similar for loss of HOH (carbocation acidity) and MeOR (=Me) (corners 1 and 3). We include the molarity of water because water is lost from the protonated alcohol for pK_{R+}, but in acetal hydrolyses 1 M alcohol is lost from protonated substrate. Values of pK_{R+} are estimated in strongly acidic solvents from 1 to 10 M acid, and the water molarity will be on the order of 20−55.5 M, which means that pK_{R+} is more negative by 3 (ln 20) to 4 (ln 55.5) units. We therefore assume that pK_{R+} for hypothetical formation of the acetal from the oxocarbenium ion and MeOH ca. −7, and the free energy for formation of oxocarbenium ion from the acetal is $\Delta\Delta G°$ (corner 1 to 3) ≈ 9.5 kcal/mol at 25 °C. Finally, $\Delta\Delta G°$ for formation of the oxocarbenium ion and MeO^-, corner 4, is the sum of $\Delta\Delta G°$ values for formation of intermediates at corner 3 from corner 1 and corner 4 from corner 3, i.e., 9.5 + 9.2, and $\Delta\Delta G°$ (corner 1 to 4) ≈ 18.7 kcal/mol. In sum, the approximate $\Delta\Delta G°$ values of species at corners 2−4 relative to corner 1 are 9.5, 9.5, and 18.7 kcal/mol, respectively. These $\Delta\Delta G°$ values are also shown in Figure 7. They indicate, qualitatively, the relative free energies of the hypothetical intermediates and are consistent with the transition state not having extensive oxocarbenium character, i.e., contributions from corners 3 and 4.

SCHEME 4

$$R^+ + H_2O \xrightleftharpoons{pK_{R+}} ROH + H_3O^+$$

The similarity of $\Delta\Delta G°$ values at corners 2 and 3 for BMA is probably fortuitous, but it is consistent with the idea that oxocarbenium formation from BMA and BBA involves extensive, although not necessarily complete, proton transfer, consistent with there being no indication of buffer catalysis of these reactions, and that relatively modest structural changes could promote the general-acid pathway. These comparisons indicate a "late" transition state. The free energy of the protonated acetal, corner 2, is much higher than that of the reactants, corner 1, thus the reaction coordinate for hydrolyses of the primary acetals should be near the right-hand side of the diagram and the transition state should be between species at corners 2 and 3 (Figure 7). The absence of observed general-acid catalysis in hydrolyses of the primary acetals BMA and BBA is consistent with rate-limiting cleavage of the protonated substrate,[3−5,15] but a concerted pathway with almost complete proton transfer in the transition state, i.e., α between 0.8 and 1,[15] cannot be distinguished kinetically. The free energies of activation, calculated by use of the Eyring equation, are 15.8 and 10.9 kcal·mol^{-1} for hydrogen-ion-catalyzed hydrolyses of BMA and BTBA, respectively. The value for hydrolysis of BMA is higher than the estimated free energies of protonated MBA and the oxocarbenium ion, as expected for a stepwise reaction. If we assume that basicities of BMA and BTBA are similar, the free energy of activation for hydrolysis of BTBA is lower than that of protonated substrate, consistent with a concerted reaction, but higher than that of the putative oxocarbenium ion product; i.e., the free energy of activation is higher than the predicted free energy of the intermediate.

The Jencks−More−O'Ferrall diagram is for a methoxy derivative, and increasing the bulk of the alkoxy groups should affect free energies of the structures at corners 1−4 to different extents. Relative to the products, corner 3, the free energy of the initial state, corner 1, should increase because of steric interactions between the alkoxy and phenyl groups. Increasing the bulk of the alkoxy groups will also destabilize the species at corner 2 by steric crowding and steric hindrance to hydration of the protonated acetal, and also destabilize the oxocarbenium ion, corner 3, although to a lesser extent because hydration of the protonated substrate, corner 2, should be stronger than that of the charge-dispersed oxocarbenium ion, corner 3. The free energy of the species at corner 4 will be increased to some extent by steric hindrance to hydration of the alkoxide ion but there should be release of steric strain in going from an sp^3 to an sp^2 carbon at the reaction center. In any event, $\Delta\Delta G°$ at this corner is much higher than at corners 2 and 3 and uncertainties in structural effects on the energy at corner 4 should not affect interpretation of the results.

In general, increasing the bulk of the alkoxy groups increases the energy of the species at corners 1 and 2 relative to 3 and 4 and the transition state moves toward the initial state along the reaction coordinate (toward corner 1 from 3) and orthogonal to the diagonal (toward corner 4 from 2).[2] This movement of the transition state is consistent with a decrease in α as observed for

(34) Bunton, C. A.; DeWolfe, R. H. *J. Org. Chem.* **1965**, *30*, 1371−1375.
(35) Ballinger, P.; Long, F. A. *J. Am. Chem. Soc.* **1960**, *82*, 795−798.
(36) Coetzee, J. F.; Ritchie, C. D. *Solute−Solvent Interactions*; Marcel Dekker: New York, 1969.

hydrolyses of secondary and tertiary acetals and increases in the rate constants corresponding to "earlier" transition states along the curved pathway in Figure 7. There should be limited oxocarbenium ion character in these transition states, consistent with a relatively low sensitivity to electronic donation from para-substituents on the phenyl group, which follows σ instead of σ^+ Hammett substituent parameters.[3,6] In addition, ρ values are significantly less negative than for S_N1 reactions of nonionic substrates.[2] Thus, proton transfer rather than C−O cleavage, is a significant source of the energy barrier in hydrolyses of primary, secondary, and tertiary acetals that can be regarded as S_E2 reactions in which an oxocarbenium ion is displaced by attack on oxygen with varying extents of bond making and breaking, Our conclusions differ from those of Jensen et al. who examined the effect of substituents in the primary alkoxy groups in terms of Taft's electronic and steric parmeters.[37] They concluded that the transition states had extensive oxocarbenium ion character, but Taft's parameters contain a mixture of electronic and steric contributions that are difficult to separate unambiguously in terms of their contributions to C−O bond cleavage and proton transfer to the alkoxy oxygen in the transition state.

Values of α for the secondary alkyl derivatives are essentially the same as those of the tertiary derivatives, although the latter are significantly more reactive (Tables 1 and 2). Apparently, increasing the bulk of these alkyl groups has little effect on the extent of proton transfer but significantly increases that of C−O bond cleavage; i.e., the transition state shifts toward the bottom side of the diagram, consistent with an increase in the energies at corners 1 and 2 relative to 3 and 4 in Figure 7.

Steric and Electronic Effects on Reactivity. Steric, rather than electronic, effects appear to be primarily responsible for the increase in reactivity in going from methyl to *tert*-alkyl derivatives (Tables 1, 2, and 4 and Figure 6). The steric parameter, ν, for alkoxy groups, developed by Charton, is based on van der Waals radii of the constituent atoms and therefore should be free of complications caused by mixing of electronic and steric effects that may contribute to other steric parameters obtained from structure−reactivity correlations.[29,30] The plot of log k_H^R/k_H^{Me} against ν (Figure 6) is linear (cc = 0.989) with a slope of ca. 2, which is clear evidence for the role of steric effects in controlling reactivity and a gradual change in extents of bond making and breaking in the transition state, but we have to consider how they may mediate electronic effects of the alkoxy groups.

In a simple acetal, the anomeric effect controls initial state conformation because of stabilizing interactions between the oxygen lone pairs, but introduction of a substituent at the reaction center, such as the phenyl group in these experiments, may generate steric interactions that decrease the oxygen−oxygen electronic interaction.[18] Chang and Su recently analyzed the factors contributing to the anomeric effect.[38] The situation is particularly complex with a phenyl substituent, which not only affects the initial state conformation but also inhibits proton transfer by an inductive effect and assists C−O bond breaking by an electronic effect. Protonation and formation of oxocarbenium ions have been treated theoretically for hydrolyses of simple acetals,[39−41] but the phenyl group introduces complicating steric interactions, and it may also stabilize a forming oxocarbenium ion to an extent that depends on the torsional angle between it and the breaking bond. However, the resonance (mesomeric) effect is not all important because electronic effects follow σ rather than σ^+ parameters in Hammett plots of acetal hydrolyses.[3] In sum, increasing the alkyl group bulk accelerates these reactions and alters extents of proton transfer and C−O bond breaking in the transition state. However, ascribing these effects to simple relief of initial state steric strain, as in S_N1 reactions of congested alkyl derivatives,[2] is probably too simplistic in view of steric effects upon the ^{13}C NMR chemical shifts and C−H coupling constants discussed below.

NMR Spectra. Both ^{13}C and ^1H NMR spectra are consistent with structures of the acetals as regards chemical shifts and multiplicities of the aliphatic groups (see Supporting Information). In addition, variations in the NMR parameters of the central (α-) C−H atoms are informative as regards initial state conformations and reactivities. Plots of ^{13}C chemical shifts, δ, and $^1J_{CH}$ against ν for the alkoxy groups are linear,[18,42] as are log k values (Figure 6). There is extensive evidence that, for acetals of aliphatic aldehydes, ^{13}C chemical shifts and $^1J_{CH}$ coupling constants at the central (α-) C−H decrease with the increasing steric bulk of the alkoxy groups. This decrease in chemical shift is associated with an increase in electron density at the reaction center, which favors development of a cationic center in transition state formation, consistent with observed increases in reactivities. The changes in coupling constants are related to changes in the dihedral angles between C−H and the oxygen unshared lone pairs, induced by the anomeric effect, and steric repulsions between alkyl groups on oxygen and the substituent on the central carbon. In contrast to the ^{13}C NMR spectra, ^1H NMR chemical shifts increase with the increasing bulk of the alkoxy groups (Figure 6), possibly due to changing orientations of the phenyl group with respect to the axis of the C−H bond induced by steric interactions with an alkoxy group, as discussed above. Interference between a *tert*-alkoxy group and phenyl group will orient the ring in line with the C−H bond generating downfield shifts, whereas orientation toward the face of the phenyl group gives upfield shifts because of interactions with the ring current of the phenyl group. This question will be discussed in a separate paper.

Conclusions

Steric bulk in the alkoxy groups accelerates acid hydrolyses. For primary alkyl groups the proton is extensively or completely transferred in the transition state, but general-acid catalysis of hydrolyses of second-

(37) Jensen, J. L.; Herold, L. R.; Lenz, P. A.; Trusty, S.; Sergi, V.; Bell, A. T.; Rogers, P. *J. Am. Chem. Soc.* **1979**, *101*, 4672−4677.
(38) Chang, Y.-P.; Su, T.-M. *J. Phys. Chem. A* **1999**, *103*, 8706−8715.
(39) Woods, R. J.; Andrews, C. W.; Bowen, J. P. *J. Am. Chem. Soc.* **1992**, *114*, 859−864.
(40) Webster, A. C.; Fraser-Reid, B.; Bowen, J. P. *J. Am. Chem. Soc.* **1991**, *113*, 8293−8298.
(41) Liang, G. Y.; Sorensen, J. B.; Whitmire, D. *J. Compt. Chem.* **2000**, *21*, 329−339.
(42) Pihlaja, K.; Nurmi, T. *Isr. J. Chem.* **1980**, *20*, 160−167.

ary and tertiary derivatives indicates concerted proton transfer and C−O bond breaking. The totality of our results is consistent with rate-determining acetal hydrolysis followed by rapid breakdown of the hemiacetal intermediate from pH 3.6−7 and at all buffer concentrations. Consideration of probable reaction paths in terms of a Jencks−More−O'Ferrall free energy diagram indicates that there is significant proton transfer in the transition state and limited buildup of positive charge at the reaction center, consistent with evidence on electronic substituent effects.[3] Steric effects upon ^{13}C chemical shifts at the central carbon show that induced changes in electron densities should affect reactivities and that accelerations are not due solely to relief of steric strain involving the alkoxy groups and changes from tetrahedral to trigonal geometries at the reaction center.

Experimental Section

Materials. Analytical grade reagents: glacial acetic acid, 40% aqueous formic acid, succinic acid, 85% phosphoric acid, potassium hydroxide, potassium chloride, anhydrous Et_2O and MeCN, $CDCl_3$ and C_2D_6OD were used as received. Aqueous solutions were prepared with either doubly distilled or Millipore treated water.

Acetals were prepared from α,α-dichlorotoluene and the corresponding alcohol by the method of Cawley and Westheimer.[16] One-half equivalent of α,α-dichlorotoluene was added dropwise to a solution of the potassium alkoxide in its alcohol, which was refluxed for 5−7 h. Excess alcohol was distilled off, the acetal was extracted into Et_2O, the mixture was filtered, and Et_2O was evaporated, and the residual oil was vacuum distilled. The ^1H and ^{13}C spectra of the acetals were consistent with their structures with no stray peaks **(**Supporting Information). The GLC chromatograms for each acetal were single peaks and their MS spectra are consistent with their structures (Supporting Information). We did not see molecular ions in the mass spectra. The highest *m/e* peaks correspond to formation of oxocarbenium ions by loss of RO, and the base peaks correspond to subsequent loss of C_nH_{2n} where *n* is the number of carbons in the alkyl groups. The 200 ^1H NMR spectrum of the sample BTBA that had been used earlier in the experiments reported here showed that it had decomposed significantly with time, as indicated by the presence of signals for both *tert*-butyl alcohol, benzaldehyde, and unidentified signals that were absent in the freshly prepared BTBA sample. BTBA was resynthesized recently, and values of k_{obs} measured under a few different buffer conditions reproduced those obtained earlier. It appears that it is desirable to use freshly prepared samples of the tertiary alkoxy acetals.

Buffer solutions were prepared by dissolving weighed amounts of the acid and KCl in water (ca. 20 mL), titrating the solution with ca. 0.9 M KOH to the desired pH and then diluting with water to 25 mL. The pH was remeasured before each experiment.

Methods. ^1H (200 MHz) and ^{13}C (50.27 MHz) NMR spectra were obtained at 25 °C in $CDCl_3$ with TMS as the internal standard. ^{13}C spectra of BTBA, BIPA, and BBA are almost identical in C_2D_6OD, showing that there are no specific solvent effects on chemical shifts. Mass spectral data were obtained on a GC−MS instrument by injecting acetals in CH_2Cl_2 onto a CBP1 (nonpolar) column (25 cm length, i.d. 0.22 mm, 0.25 mm particle size) using a temperature gradient of 40−310 °C at 10 °C/min followed by 5 min at 310 °C and a 70 V EI source at 25 ° C. Hydrolyses were followed on a diode array spectrophotometer, and pH was measured on a potentiometer.

Kinetics. A stock solution (10 μL of acetal, 8.0×10^{-3} M in dry MeCN) was injected into 2 mL of aqueous buffer (see preparation above) at 25.0 °C. Reactions were followed at 250 nm for at least 10 half-lives. Rate constants were calculated from data obtained over 4−5 half-lives by Guggenheim's method with HP-89532-K kinetic software. Rate constants were determined in triplicate with <5% deviations.

pK_a Determinations. The pK_a values of formic and acetic acids were determined by potentiometric titration. A 0.1 M solution of the acid containing 0.5 M KCl was titrated with standardized 1.02 M NaOH in 0.5 M KCl. The pK_a was obtained from the inflection point of the pH−volume NaOH solution curves.

Acknowledgment. D.Z. is grateful for financial support from PRONEX and CNPq, 910039/97-6, which provided support the Brasil-USA collaboration. C.A.B. and L.S.R. are grateful for support from the National Science Foundation U. S.-Brasil Cooperative Science Program (INT-9722458). L.S.R. thanks Lata Rachakonda for patient word processing, Eric Romsted for assistance in the analysis of kinetic data, and NSF (CHE-9985774) for financial support.

Supporting Information Available: Seventeen tables containing (a) the complete set of buffer catalysis data used to estimate the second-order rate constants for the hydronium ion and buffer-catalyzed reactions for the hydrolyses of all primary, secondary, and tertiary dialkyl benzaldehyde acetals, (b) Brønsted α values for secondary and tertiary dialkyl benzaldehyde acetals comparing three methods of calculating α, and (c) the ^{13}C and ^1H NMR and GC−MS analytical data on the acetals. This material is available free of charge via the Internet at http://pubs.acs.org.

Appendix

This appendix summarizes the processes and mathematical derivations for estimating the rate constants for general-acid catalysis of acetal hydrolysis for the di- and monoacid forms of succinic acid by Methods I and II. The original data for these calculations is in the Supporting Information. The final values of the rate constants for both methods are listed in Table 2 in the text.

Method I. The process is divided into two steps: (a) obtaining initial estimates of the rate constants by using simplified forms of the full rate expression and (b) using the initial estimates in an iterative process to obtain more accurate values of each rate constant. In general, for each secondary and tertiary acetal value of k_{HA} were obtained from k_{obs} values measured at the one or two highest pH values and values of k_{H_2A} were obtained from the one or two lowest pH values measured. The decision of what values to use was based on data quality, i.e., the correlation coefficients of the plots.

1. Estimating k_{HA}. The full rate expression for general-acid catalysis by succinic acid is

$$k_{obs} = k_H[H_3O^+] + k_{HA}[HA^-] + k_{H_2A}[H_2A] \quad (A1)$$

To obtain an initial estimate of k_{HA}, we assume that at the highest pH used $k_{H_2A}[H_2A] \approx 0$ to give

$$k_{obs} = k_H[H_3O^+] + k_{HA}[HA^-] \quad (A2)$$

Equation A2 is rearranged to give

$$\frac{k_{obs}}{[H_3O^+]} = k_H + \frac{k_{HA}[HA^-]}{[H_3O^+]} \quad (A3)$$

The value of k_{obs} is measured and the value of $[H_3O^+]$ is obtained from the measured pH. The value of $[HA^-]$ at a particular pH is obtained by solution of a quadratic expression (see below).

To obtain a refined value of k_{HA} by iteration, eq A1 is combined with the expression for the acidity constant of succinic acid, eq A4, and rearranged to give eq A5:

$$K_a(1) = \frac{[HA^-][H_3O^+]}{[H_2A]} \quad \text{(A4)}$$

$$Y(k_{HA}) = \frac{k_{obs}}{[H_3O^+]} - \frac{k_{H_2A}[HA]}{K_a(1)} = k_H + \frac{k_{HA}[HA^-]}{[H_3O^+]} \quad \text{(A5)}$$

and $Y(k_{HA})$, which is equal to the next equality, is plotted against $[HA^-]/[H_3O^+]$, with the slope = k_{HA} and the intercept = k_H.

2. Estimating k_{H_2A}. To obtain an initial estimate of k_{H_2A}, we assume that at the lowest pH used $k_{HA}[HA^-] \approx 0$ and eq A1 becomes

$$k_{obs} = k_H[H_3O^+] + k_{H_2A}[H_2A] \quad \text{(A6)}$$

Equation A6 is rearranged to

$$\frac{k_{obs}}{[H_3O^+]} = k_H + \frac{k_{H_2A}[H_2A]}{[H_3O^+]} \quad \text{(A7)}$$

The value k_{obs} is measured and the value of $[H_3O^+]$ is obtained from the measured pH. The value of $[H_2A]$ at a particular pH is obtained by solution of a quadratic expression (see below).

To obtain a refined value of k_{H_2A} by iteration, eq A1 was rearranged to give

$$Y(k_{H_2A}) = \frac{k_{obs}}{[H_3O^+]} - \frac{k_{HA}[HA]}{[H_3O^+]} = k_H + \frac{k_{H_2A}[H_2A]}{[H_3O^+]} \quad \text{(A8)}$$

and $Y(k_{H_2A})$, which is equal to the next equality, is plotted against $[H_2A]/[H_3O^+]$, with the slope = k_{H_2A} and the intercept = k_H.

3. Iterative Procedure. The first iteration of eq A5, in which the initial estimate of k_{H_2A} is obtained from eq A7, gives a value of k_{HA}. The concentrations of HA^-, H_2A, and A^{2-} are obtained from quadratic equations for their concentrations by using the first and second pK_a values for succinic acid (see below). The value of k_{HA} obtained from eq A5 is then plugged into eq A8 to give the first iterative estimate of k_{H_2A}. This value of k_{H_2A} is then plugged back into eq A5 to obtain the second iterative estimate of k_{HA}. This process is repeated until the separate values of k_{HA} and k_{H_2A} converge, which usually takes four iterations.

4. Derivation of Quadratic Equations for the Diacid, H_2A, and Monoacid, HA^-, Forms of Succinic Acid in Terms of the Total Stoichiometric Succinic Acid Concentration, A_T. (a) Derivation of the Concentration of H_2A. The expressions for the acidity constants are substituted into the mass balance equation for succinic acid

$$[A_T] = [H_2A] + [HA^-] + [A^{2-}] \quad \text{(A9)}$$

to give

$$[A_T] = [H_2A] + \frac{[H_2A]K_a(1)}{[H_3O^+]} + \frac{[HA^-]K_a(2)}{[H_3O^+]} \quad \text{(A10)}$$

Substitution for $[HA^-]$ gives

$$[A_T] = [H_2A] + \frac{[H_2A]K_a(1)}{[H_3O^+]} + \frac{[H_2A]K_a(1)\,K_a(2)}{[H_3O^+]^2} \quad \text{(A11)}$$

Solving for $[H_2A]$ gives

$$[H_2A] = \frac{[A_T][H_3O^+]}{[H_3O^+]^2 + K_a(1)[H_3O^+] + K_a(1)\,K_a(2)} \quad \text{(A12)}$$

(b) Derivation of the Concentration of HA^-. The expressions for the acidity constants are substituted into eq A9 to give

$$[A_T] = \frac{[H_3O^+][HA^-]}{K_a(1)} + [HA^-] + \frac{K_a(2)[HA^-]}{[H_3O^+]} \quad \text{(A13)}$$

Equation A13 is solved for $[HA^-]$:

$$[HA^-] = \frac{[A_T][H_3O^+]K_a(1)}{[H_3O^+]^2 + [H_3O^+]K_a(1) + K_a(1)K_a(2)} \quad \text{(A14)}$$

Method II. To check on the quality of estimates of k_{HA} and k_{H_2A} obtained by method I, we also estimated these constants by a second method based on difference.

To estimate k_{H_2A}, the definition of the first acidity constant $K_a(1)$ for succinic acid was combined with the mass balance equation

$$K_a(1) = \frac{[HA^-][H_3O^+]}{[H_2A]} \quad \text{(A15)}$$

$$[A_T] = [H_2A] + [HA^-] \quad \text{(A16)}$$

to give eq A17, which was used to solve for $[H_2A]$ at the lowest or two lowest pH values used, assuming that $[HA^-]$ was negligible because k_{HA} is about 10 times smaller than k_{H_2A} (see Table 2 in the text). The values of

$$[H_2A] = \frac{[A_T][H_3O^+]}{K_a(1) + [H_3O^+]} \quad \text{(A17)}$$

$[H_2A]$ at each buffer concentration were substituted into eq A18 and values of k_{H_2A} were obtained from the slope of $k_{obs} - k_H(av)[H_3O^+]$ vs $[H_2A]$, where $k_H(av)$ is the average value of k_H obtained from values of k_H from the intercepts of plots using the other buffers, e.g., formate, acetate, and phosphate (see Table 2 in text).

$$k_{obs} - k_H(av)[H_3O^+] = k_{H_2A}[H_2A] \quad \text{(A18)}$$

To estimate k_{H_2A}, the definition of the second acidity constant $K_a(2)$ for succinic acid, eq A19, was combined

with the mass balance equation (eq A20), to give eq A21,

$$K_a(2) = \frac{[A^{2-}][H_3O^+]}{[HA^-]} \quad \text{(A19)}$$

$$[A_T] = [HA^-] + [A^{2-}] \quad \text{(A20)}$$

which was used to solve for $[HA^-]$ at the two lowest pH values used, assuming that $[H_2A]$ was negligible. The

$$[HA^-] = \frac{[A_T][H_3O^+]}{K_a(2) + [H_3O^+]} \quad \text{(A21)}$$

values of $[HA^-]$ at each buffer concentration were substituted into eq A22 and values of k_{HA} were obtained from the slope of $k_{obs} - k_H(av)[H_3O^+] - k_{H_2A}[H_2A]$ vs $[HA^-]$.

$$k_{obs} - k_H(av)[H_3O^+] - k_{H_2A}[H_2A] = k_{HA}[HA^-] \quad \text{(A22)}$$

JO0202987